ORIGINALE ARTICLE

SIMULATION OF PALLADIUM GROWTH BY CLASSICAL MOLECULAR DYNAMIC

| Dimbimalala, Randrianasoloharisoa [1*] | Iando, Rinah Razafinjatovo [1] | and | Fils, Lahatra Razafindramisa [1] |

[1.] Université d'Antananarivo | Département de Physique | Laboratoire de Physique de la Matière et du Rayonnement | Antananarivo | Madagascar |

| Received July 29, 2023 | | Accepted September 07, 2023 | | Published September 09 2023 | | ID Article | Dimbimalala-Ref2-2-17ajiras290823 |

ABSTRACT

Background: Palladium is a metal with numerous intriguing applications, particularly in catalysis, owing to its unique electronic properties. These electronic and catalytic characteristics are significantly influenced by its crystallographic structure. Palladium possesses a face-centered cubic (fcc) structure. **Objectives**: The principal aim of this study is to investigate the impact of temperature on the structure formed when palladium shells are deposited onto a palladium substrate. **Methods**: We employed the classical molecular dynamics method to simulate the growth process and determine the structure of the layers formed as atoms are deposited individually. The atomic interactions within the system were represented by the Embedded Atom Method (EAM) potential. Our approach involved constructing substrates, each composed of five layers of palladium oriented in the (111) direction. These various substrates were then subjected to different temperatures ranging from 150K to 1000K. Palladium atoms were subsequently deposited onto the substrates to create layers, and the interlayer and interatomic distances were assessed to determine the structure of the deposited layers. **Results**: In general, as temperature increases, both interlayer distances of substrates and adatoms also increase. Conversely, for adatoms, this distance decreases as one moves from the inner layers towards the surface layers at each temperature, converging toward the value of bulk palladium. Regarding interatomic distances, our results indicate that they increase with temperature, but they remain in close proximity to the distances observed in solid palladium. Analysis of the atomic arrangements reveals a tendency towards obtaining more fcc structures as the temperature rises. **Conclusions**: This study has provided insights into the influence of temperature on the formation of fcc structures during the deposition of palladium layers. The findings demonstrate that higher temperatures lead to increased distances between layers and atoms. Nevertheless, these distances remain similar to those found in solid palladium. Additionally, the rise in temperature promotes the prevalence of fcc structures at the expense of hcp structures.

Keywords: *Thin films, thin layers, Embedded Atom Method.*

1. INTRODUCTION

In today's world, the field of surface physics and the study of thin layers are experiencing remarkable growth due to their numerous and diverse applications, such as electronics and microelectronics, catalysis, magnetism, and metallurgy. Many studies have concentrated on the development and application of thin films or layers of these materials, as they often exhibit exceptional structural and physical properties distinct from those in their bulk state. For instance, refer to [1, 2, 3]. Experimental research involves the production and characterization of thin films to comprehend their characteristics and properties. In contrast, theoretical studies rely on solid-state physics and crystallography, with their role being to model the system (the film) and interpret experimental results. The emergence and evolution of increasingly powerful computers have also opened up another avenue for studying thin films: numerical simulation.

In this research, we will conduct numerical simulations of palladium-based thin-film systems to gain insights into various parameters, particularly temperature, which can affect the face-centered cubic (fcc) structure of palladium. Our goal is to achieve a palladium layer without altering the fcc structure. It's worth noting that palladium is a highly sought-after metal due to its remarkable physical and chemical properties. It finds applications in various industries, such as electronics and electrical, where it's used in the production of cell phones, computers, fax machines, dental prosthetics in the form of various alloys with copper, silver, gold, platinum, and even zinc, jewelry, where it contributes to the composition of white gold, and catalytic converters, which are a significant application today. In the chemical industry, it accounts for 5% of its global consumption and is used, for instance, as a catalyst in hydrogenation or dehydrogenation reactions, such as in petroleum cracking. Palladium also serves as an excellent electro-catalyst for the oxidation of primary alcohols in an alkaline medium [4]. However, the primary consumer of palladium is the automotive industry [5]. Palladium is indeed used, along with other compounds like platinum and rhodium, in catalytic converters to expedite the conversion of toxic products resulting from fuel combustion (carbon monoxide and nitrogen oxides) into less harmful compounds: CO2 and water [6]. This sector accounted for 57% of estimated global consumption in 2006 and over 80% in 2018 [5]. Finally, its ability to capture dihydrogen holds potential applications in the energy sector."

2. MATERIALS AND METHODS

Our work consists in studying by molecular dynamics the mechanism of growth and the structure of palladium.

*Corresponding author Author & Copyright Author © 2023: | Dimbimalala, Randrianasoloharisoa * |. All Rights Reserved. All articles published in *the American Journal of Innovative Research and Applied Sciences* are the property of Atlantic Center Research Sciences, and is protected by copyright laws CC-BY. See: http://creativecommons.org/licenses/by-nc/4.0/.

2.1 Systems studied

The system we studied consists of a palladium substrate on which layers of palladium are deposited. The substrate is formed of 5 layers, the surface of which is oriented (111). The 2 lower layers are kept fixed to preserve the orientation of the surface while the 3 upper ones can move to take into account the temperature. Each layer of the substrate is made up of 400 atoms, ie 2000 atoms in total for the 5 layers. The deposition of the layers consists in throwing one by one on the substrate the atoms which will spread out to form the layers. The initial energy of the atom to be deposited is 1eV. The lattice parameter of palladium is 3.89Å. We made simulations for different temperatures of the substrate: 150°K, 300°K, 600°K, 900°K and 1000°K.

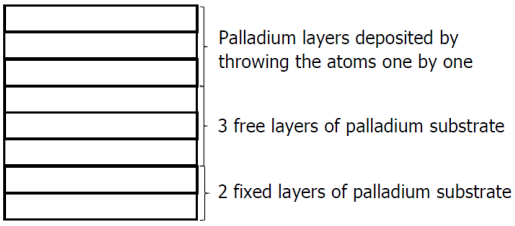

Figure 1: The figure schematically shows the studied system.

2.2 Simulation method

The use of molecular dynamics (MD) methods dates back to the 1950s, and interest in these techniques continues to grow in the field of materials science. Despite recent advances, accessing the atomic scale experimentally remains challenging in many fields. Atomic-scale simulations, and molecular dynamics in particular, are, therefore, highly valuable investigative tools. In this study, we employed numerical simulation through classical Molecular Dynamics based on Verlet's algorithm [7]. The Molecular Dynamics method involves tracking the movement of each atom constituting the system by solving Newton's equations of motion. For a particle i, we have [8,9]:

$$\vec{f_i} = m_i \vec{\gamma}_i \quad \textbf{(1)}$$

$\vec{f_i}$ is the applied force to atom i, m_i the mass of atom i and $\vec{\gamma}_i(t)$ the acceleration of atom i at time t:

$$=> \ \vec{f_i} = m_i \frac{d^2\vec{r}_i(t)}{dt^2} \quad \textbf{(2)}$$

$\vec{r}_i(t)$ is the position of atom i at time t

$$=> \ \frac{\vec{f}_i}{m_i} = \frac{d^2\vec{r}_i(t)}{dt^2} \quad \textbf{(3)}$$

Solving equation (3) gives the different positions $\vec{r}_i(t)$ of particle i as a function of time. For this we can do the Taylor series expansion of order 4 of $\vec{r}_i(t+\Delta t)$ and $\vec{r}_i(t-\Delta t)$:

$$\vec{r}_i(t+\Delta t) = \vec{r}_i(t) + \frac{d\vec{r}_i(t)}{dt}\Delta t + \frac{1}{2!}\frac{d^2\vec{r}_i(t)}{dt^2}\Delta t^2 + \frac{1}{3!}\frac{d^3\vec{r}_i(t)}{dt^3}\Delta t^3 + O(\Delta t^4) \quad \textbf{(4)}$$

$$=> \ \vec{r}_i(t+\Delta t) = \vec{r}_i(t) + \frac{d\vec{r}_i(t)}{dt}\Delta t + \frac{1}{2}\frac{\vec{f}_i(t)}{m_i}\Delta t^2 + \frac{1}{6}\frac{d^3\vec{r}_i(t)}{dt^3}\Delta t^3 + O(\Delta t^4) \quad \textbf{(5)}$$

$$\text{and } \vec{r}_i(t-\Delta t) = \vec{r}_i(t) - \frac{d\vec{r}_i(t)}{dt}\Delta t + \frac{1}{2}\frac{\vec{f}_i(t)}{m_i}\Delta t^2 - \frac{1}{6}\frac{d^3\vec{r}_i(t)}{dt^3}\Delta t^3 + O(\Delta t^4) \quad \textbf{(6)}$$

By adding equations (5) and (6) we have:

$$\vec{r}_i(t+\Delta t) + \vec{r}_i(t-\Delta t) = 2\vec{r}_i(t) + \frac{\vec{f}_i(t)}{m_i}\Delta t^2 + O(\Delta t^4) \quad \textbf{(7)}$$

$$=> \vec{r}_i(t+\Delta t) = 2\vec{r}_i(t) - \vec{r}_i(t-\Delta t) + \frac{\vec{f}_i(t)}{m_i}\Delta t^2 + O(\Delta t^4) \quad \textbf{(8)}$$

Equation (8) constitutes Verlet's algorithm for a particle i. With this algorithm it is possible to determine the position of each particle i at time $(t+\Delta t)$. Its application requires knowing the positions of particle i at times t and $(t-\Delta t)$ and the force applied to it at time t.

2.3 Edge effect and long-distance interaction

The number of atoms that the computer can simulate is limited. Typically, these N atoms are contained in a box with dimensions sx, sy, and sz. To simulate a crystal of pseudo-infinite size, periodic conditions are often applied to the edges of the box. Whenever an atom exits the box on one side, it re-enters from the opposite side with the same velocity. It's worth noting that periodic boundary conditions preserve the system's total momentum; this concept is known as the minimum image convention or periodic boundary condition. Essentially, the idea is to replicate each cell containing the N atoms in 2 (or 3) dimensions, depending on the study, maintaining the same relative positions for each particle. This replication creates a system of infinite size or infinite surface area in cases where replicas are made in two dimensions. Figure 2 illustrates this model, with the central gray box representing the system under study, which is then replicated in all directions.

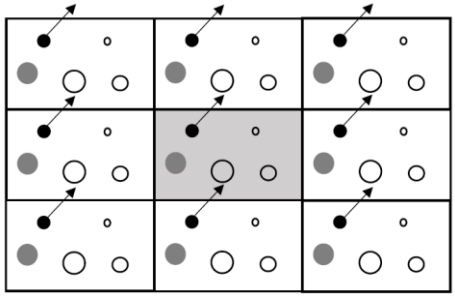

Figure 2: The figure schematically shows the periodic boundary condition.

During the simulation, when a particle moves within the original box, its periodic images in each neighboring box move in exactly the same way. Therefore, if one of the movements causes a particle, such as the black one, to exit the central box, it simultaneously results in one of its images entering the central cell. Consequently, the total number of particles remains unchanged. There is no need to store the coordinates of all image particles in a simulation; only those of the central box need to be stored. The energy of the black particle within the central box must be calculated based on interactions with all particles, including the image particles.

In general, particle interaction potentials have a very long range, as is the case for Coulomb interactions. Nevertheless, their intensities become negligible at a certain distance. This implies that when calculating the energy of a given particle, only those particles whose distance from this center is less than rc (cutoff radius) are considered. Interactions between force centers located at a distance greater than rc are not taken into account [9].

2.4 Embedded Atom Method (EAM) interatomic potential

The interatomic potential is a potential energy model used to describe interactions between atoms. The use of a potential is essential when employing the Molecular Dynamics method. The Embedded Atom Method (EAM) potential was introduced in the 1980s by Daw et al. The underlying concept of this method is to treat each atom as an impurity concerning the other atoms within the system. This potential was specifically developed for metallic systems [10].

$$E_i = \frac{1}{2}\sum_{j\neq i} \Phi_{ij}(\vec{r}_{ij}) + F(\rho_i(\vec{r}_{ij})) \qquad \textbf{(9)}\ [11]$$

In equation (9), the term $\sum_{j\neq i} \Phi_{ij}(\vec{r}_{ij})$ represents the peer interaction energies of atom i with its neighbors j separated by a distance $\vec{r}_{ij}$ and $F(\rho_i(\vec{r}_{ij}))$ is the energy required to insert this atom i into the medium where there is an electronic density $\rho_i(\vec{r}_{ij})$ created by the other atoms of this medium.

The total energy of the crystal is obtained by summing the energy of each atom, i.e.:

$$E = \frac{1}{2}\sum_{i,j(i\neq j)} \Phi_{ij}(\vec{r}_{ij}) + \sum_i F_i(\rho_i) \qquad \textbf{(10)}$$

To calculate the terms $\sum_{i,j(i\neq j)} \Phi_{ij}(\vec{r}_{ij})$, $F(\rho_i(\vec{r}_{ij}))$, and $F(\rho_i(\vec{r}_{ij}))$ we use the method proposed by Johnson et al., (2001) [12].

3. RESULTS AND INTRPRETATION

Our work is centered around the study of the Pd/Pd system, specifically involving the simulation of palladium layer deposition on a palladium substrate with a face-centered cubic structure (111). During the thin-film deposition process, the morphological properties of the film are influenced by several parameters, including adatom deposition frequency, energy, angle of incidence, and substrate temperature.

In this research, we will investigate the impact of substrate temperature on the structure of the deposited layers. We have selected the following substrate temperatures: 150 K, 300 K, 600 K, 900 K, and 1000 K.

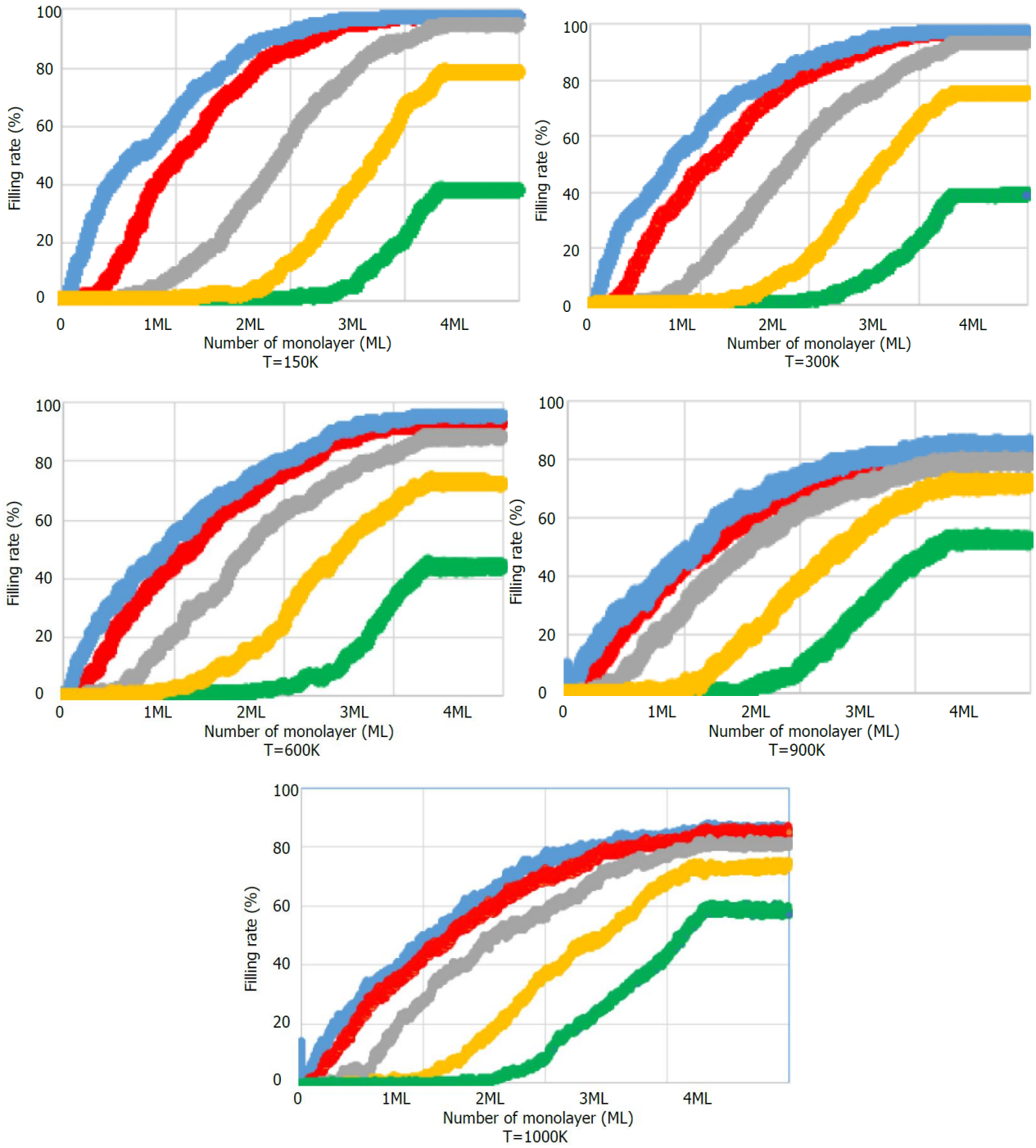

Figure 3: The figure represents the filling curves of the layers of adatoms for different temperatures. On the abscissa we have the number of monolayers (ML), i.e. the number of adatoms to fill a layer and on the ordinate we have the filling rate (in %) of the deposited layers.

Figure 3 represents the filling curve of adatom layers on the substrate. This curve illustrates the growth of each Pd monolayer (ML) on the Pd substrate. The blue curve represents the filling of the first layer, the red represents the second, the grey represents the third, the yellow represents the fourth, and the green represents the fifth. Please recall that a monolayer represents the number of atoms required to fill a layer.

The mode of filling or growth of these layers is determined by the slope of each curve and the difference between the abscissae of two adjacent curves. When the curve has a steep slope and the gap is significant, the growth mode closely resembles the Franck-Van der Merwe (2D) mode or layer-by-layer growth. In this mode, the filling of an upper layer begins only when the layer below it is completely filled. Conversely, when the gap is small, we observe Volmer-Weber-type growth (3D), where a layer begins to grow before the previous layer is completely filled.

According to Figure 3, at high temperatures, specifically 600K, 900K, and 1000K, the first and second layers are filled practically simultaneously. However, the difference in filling time increases as we move further from the substrate. This implies that in the vicinity of the substrate, atoms tend to settle on sites where islands have already formed rather than

directly on the substrate, indicating Volmer-Weber-type growth. As we move away from the substrate, adatoms start to exhibit Franck-Van der Merwe (2D) growth. But even as they grow on islands, a layer cannot be completely filled until the layer below it is full. This tendency toward 3D growth is less pronounced at substrate temperatures of 150K and 300K. However, it becomes more prominent as the substrate temperature increases. In fact, an adatom arriving on a hot substrate prefers to migrate to a colder layer of adatoms.

Table 1: The table presents coverage rate (in %) of the layers of adatoms deposited according to the temperatures. The 1st layer is the layer just above the substrate and the 5th layer is the layer on the surface.

	T=150K	T=300K	T=600K	T=900K	T=1000K
4th layer	78.25	75.25	72.5	72.25	74
3rd layer	94.25	92.75	88	78.5	81.5
2nd layer	97.5	97.25	92.5	82.75	85
1st layer	97.5	97.5	95.5	84.5	85.5

Table 1 summarizes the variation in the filling rate of a monolayer as a function of temperature. From Table 1, it is evident that the filling ratio of each layer decreases, indicating an increase in vacancies as one progresses to the upper layers. Indeed, the upper layers cannot be filled if the layers below them are not. The filling rates of the upper layers are either less than or equal to those of the lower layers. Similarly, the filling ratio decreases with increasing temperature. This is because temperature enhances the mobility of atoms, leading to the formation of gaps between atoms. However, even at high temperatures, specifically 600K, 900K, and 1000K, the filling rate of the lower layers remains high, ranging from 85.5% to 95.5% for the 1st layer and from 82.75% to 92.5% for the second layer. It's important to note that, as we observed in the filling curves in Figure 3, the growth of these first two layers follows the Volmer-Weber type, where the filling of the 1st layer is not yet complete when the 2nd layer begins to grow. Nevertheless, by the end, we find that the 1st layer is nearly filled, indicating that atoms on the formed islands migrate towards the gaps in the lower layers. This migration is possible due to the increased energy of the atoms with rising temperature.

In the following sections, we present the computational results of various parameters used to characterize the structures obtained at the end of the molecular dynamics simulations. We will examine the variation in interatomic distance and the variation in interlayer distance as functions of the changing substrate temperature.

The interlayer distance at the substrate level obtained from the simulation is provided in Table 2. This distance represents the spacing between two consecutive layers. Please remember that the substrate consists of five layers.

Table 2: The table presents distance between 2 adjacent layers (in Å) of the substrate layers according to the temperatures. The 1st layer is the lowest and the 5th is the layer just below the adatoms.

distance between 2 adjacent layers	T=150K	T=300K	T=600K	T=900K	T=1000K
4th-5th layer	2.30	2.31	2.31	2.37	2.39
3rd-4th layer	2.32	2.32	2.33	2.41	2.39
2nd-3rd layer	2.32	2.32	2.33	2.38	2.37
1st-2nd layer	2.25	2.25	2.25	2.25	2.25

The lattice parameter of solid palladium is 3.89Å which gives an interlayer distance of 2.24Å according to the orientation (111). From table 2, we can see that this distance increases with temperature, resulting in a widening of the substrate layers. The deposition of a thin layer on a substrate thus causes deformation in the arrangement of the substrate atoms.

Table 3: The table presents distance between 2 adjacent layers (in Å) of the adatom layers according to the temperatures.

distance between 2 adjacent layers	T=150K	T=300K	T=600K	T=900K	T=1000K
3rd-4th layer	2.23	2.24	2.23	2.26	2.26
2nd-3rd layer	2.28	2.29	2.24	2.27	2.29
1st-2nd layer	2.30	2.30	2.29	2.27	2.28
Substrate-1st layer	2.43	2.44	2.46	2.35	2.36

In Table 3, we present the simulation results for the distance between adatom layers. From these results, it's evident that interlayer distances do not vary significantly as a function of substrate temperature. Substrate temperature, therefore, exerts minimal influence on the distance between each layer during thin film deposition. It's also noteworthy that the distance between the last substrate layer and the first adatom layer is greater compared to the distance between the adatom layers. This difference arises from the interaction of the substrate with the adatoms arriving at a certain speed. Upon reaching the substrate, the incident atom undergoes a bounce before redistributing its energy to neighboring atoms, leading to the rearrangement of atoms on the surface of the substrate and the first layer of adatoms.

In Table 4, we present the interatomic distances for the deposited layers, specifically the average distance between an atom and its nearest neighbors.

Table 4: The table presents interatomic distance (in Å) of the adatom layers according to the temperatures.

	T=150K	T=300K	T=600K	T=900K	T=1000K
4th layer	2.78	2.82	2.82	2.90	2.91
3rd layer	2.77	2.80	2.81	2.88	2.88
2nd layer	2.77	2.78	2.80	2.87	2.85
1st layer	2.75	2.78	2.80	2.85	2.85

According to the results of the simulation presented in Table 4, as the temperature increases, the distance between an atom and its nearest neighbors tends to increase. Even at the same temperature, this distance increases when moving from the inner layer to the surface layer. Nevertheless, these distances remain relatively close to the calculated value, which is 2.75 Å for an oriented layer (111). This increase in distance can be described as relaxation—a process that manifests itself as a slight displacement of atoms.

According to the simulation, in addition to the face-centered cubic (fcc) structure, the hexagonal close packing (hcp) structure was observed. Table 5 summarizes the percentage of atoms adopting the hcp structure in each layer at different substrate temperatures. The coexistence of these two crystal structures can be attributed to surface reconstruction.

Table 5: The table presents the percentage of atoms with hcp structure in each deposited layer.

	T=150K	T=300K	T=600K	T=900K	T=1000K
4th layer	0	10.33	9.06	6.30	0
3rd layer	8.47	9.73	9.85	0	0
2nd layer	18.46	9.79	9.50	0	0
1st layer	10.26	6.67	5.84	0	0
Total	37.19	36.52	34.25	6.30	0

Table 5 presents the percentage of atoms adopting the hexagonal close packing (hcp) structure within each deposited layer at various substrate temperatures. The table showcases how the prevalence of the hcp structure changes with temperature:

At 150K: In the 4th layer, none of the atoms exhibit the hcp structure, while in the 3rd, 2nd, and 1st layers, there are relatively low percentages of atoms (10.33%, 9.79%, 6.67%, respectively) with the hcp structure. The total percentage of hcp-structured atoms across all layers at this temperature is 37.19%.

At 300K: The 4th layer still lacks the hcp structure, but the 3rd layer has a noticeable increase in atoms with hcp structure (9.73%). The 2nd layer also exhibits a similar percentage (9.79%), while the 1st layer shows a decrease (6.67%). The total percentage of hcp-structured atoms across all layers at this temperature is 36.52%.

At 600K: In the 4th layer, a small percentage of atoms (9.06%) now have the hcp structure. The 3rd and 2nd layers continue to have hcp-structured atoms (9.85% and 9.50%, respectively), while the 1st layer experiences a decrease (5.84%). The total percentage of hcp-structured atoms across all layers at this temperature is 34.25%.

At 900K: Interestingly, the 4th layer sees a decrease in hcp-structured atoms (6.30%). In contrast, the 3rd, 2nd, and 1st layers no longer have any atoms adopting the hcp structure. The total percentage of hcp-structured atoms across all layers at this temperature is 6.30%.

At 1000K: The hcp structure disappears entirely from all layers. The total percentage of hcp-structured atoms across all layers at this temperature is 0%.

Table 5 demonstrates that the prevalence of the hcp structure varies with temperature, diminishing as temperatures rise. As temperature increases, a higher proportion of face-centered cubic (fcc) structures forms. The elevated substrate temperature induces thermal agitation among the adatoms, increasing their mobility and improving growth quality, facilitating layer-by-layer growth without altering the initial crystalline structure.

4. CONCLUSION

In this study, we employed classical molecular dynamics to simulate the growth of palladium layers on a palladium substrate. Our objective was to investigate the growth and structure of palladium layers on a palladium substrate with a face-centered cubic structure oriented in a (111) plane. The primary focus was to examine the influence of substrate temperature on the structures of the deposited layers using the molecular dynamics algorithm. The various substrate

temperatures we utilized were 150K, 300K, 600K, 900K, and 1000K. To assess the impact of temperature, we calculated interlayer distances and interatomic distances to determine the crystallographic structures of the layers obtained.

The results obtained from the simulation revealed that a face-centered cubic structure of the deposited layers can be achieved when the substrate temperature is high, specifically at 900K and above. Increasing temperature has a minor effect on interlayer distances, whereas interatomic distances between first neighbors increase with temperature. Consequently, elevating the temperature leads to an increase in atomic mobility, causing more mobile atoms to adopt structures that minimize their energies.

6. REFERENCES

1. Alex NK. Selection of dielectrics for alternating-current thin-film electroluminescent device. *Thin Solid Films*. 1999;347(1-2):1-13.
2. James AO, Tien-Chien J. Atomic layer deposition and other thin film deposition techniques: from principles to film properties. *J Mater Res Technol*. 2022;21:2481-2514.
3. Thanka Rajan S, Subramanian B, Arockiarajan A. A comprehensive review on biocompatible thin films for biomedical application. *Ceram Int*. 2022;48(4):4377-4400.
4. Jiro T. Palladium Reagents and Catalysts: New Perspectives for the 21st Century. Wiley and Sons; 2004.
5. Tiffany H. This Metal Is Worth More Than Gold, and It Scrubs Your Car's Exhaust. The New York Times. 2018 Dec 13. Available from: https://www.nytimes.com/2018/12/13/business/palladium-worth-more-than-gold.html. Accessed 2021 Dec 30.
6. Carmen D. Palladium's Hidden Talent. Chem Eng News. 2008;86(35):53-56.
7. Pascal V. Simulation numérique en physique statistique. Cours de Master 2ème année « Physique théorique des systèmes complexes » et « Modélisation, statistique et algorithme des systèmes hors d'équilibre ». 2016. p33–45 (Chap 3). Available from: https://cel.archives-ouvertes.fr/cel-00092945.
8. Dimbimalala R, Heriniaina A, Fils LR. Etude par la dynamique moléculaire de la croissance de couches de platine. *Am J Innov Res Appl Sci*. 2020;11(3):165-172.
9. Toky HA, Dimbimalala R, Fils LR. Simulation numérique de la croissance du fer sur un substrat en cobalt et en nickel par la dynamique moléculaire. *Am J Innov Res Appl Sci.* 2022;14(6):288-294.
10. Daw MS, Baskes MI. Embedded-atom method: Derivation and application to impurities, surfaces and other defects in metals. *Phys Rev B*. 1984;29:6443.
11. Zou W, Wadley HNG, Zhou XW, Johnson RA, Brownell D. Surfactant-mediated growth of giant magnetoresistance multilayers. *Phys Rev B*. 2001;64:174418/1-10.
12. Wadley HNG, Zhou XW, Johnson RA. Atomic assembly of giant magnetoresistive multilayers. *MRS Symp Proc*. 2001;672:O4.1.1-O4.1.14.

How to cite this article: Dimbimalala Randrianasoloharisoa, Iando Rinah Razafinjatovo, and Fils Lahatra Razafindramisa. SIMULATION OF PALLADIUM GROWTH BY CLASSICAL MOLECULAR DYNAMIC. *Am. J. innov. res. appl. sci.* 2023; 17(3): 176-182.

This is an Open Access article distributed in accordance with the Creative Commons Attribution Non Commercial (CC BY-NC 4.0) license, which permits others to distribute, remix, adapt, build upon this work non-commercially, and license their derivative works on different terms, provided the original work is properly cited and the use is non-commercial. See: http://creativecommons.org/licenses/by-nc/4.0/